Katholieke Universiteit Leuven

Departement Elektrotechniek ESAT-SISTA/TR 2002-118

Bitrate Maximizing Time-Domain Equalizer Design for DMT-based Systems [1]

Koen Vanbleu, Geert Ysebaert, Gert Cuypers and Marc Moonen [2], Katleen Van Acker[3][4]

Published in *IEEE Transactions in Communications*, vol. 52, no. 6, pp. 871-876, June 2004.

[1]This report is available by anonymous ftp from *ftp.esat.kuleuven.ac.be* in the directory *pub/sista/vanbleu/reports/02-117.ps.gz*

[2]K.U.Leuven, Dept. of Electrical Engineering (ESAT), Research group SCD, Kasteelpark Arenberg 10, 3001 Leuven-Heverlee, Belgium, Tel. 32/16/32 18 41, Fax 32/16/32 19 70, WWW: *http://www.esat.kuleuven.ac.be/sista*. E-mail: *koen.vanbleu@esat.kuleuven.ac.be*. Koen Vanbleu is a Research Assistant supported by the Fonds voor Wetenschappelij k Onderzoek (FWO) - Vlaanderen. Geert Ysebaert and Gert Cuypers are Research Assistants supported by I.W.T.

[3]Access to Networks, Research and Innovation, ALCATEL, 2018 Antwerpen, Belgium

[4]This research work was carried out at the ESAT laboratory of the Katholieke Universiteit Leuven, in the frame of the Belgian State, Prime Minister's Office - Federal Office for Scientific, Technical and Cultural Affairs - Interuniversity Poles of Attraction Programme (2002-2007) - IUAP P5/22 ('Dynamical Systems and Control: Computation, Identification and Modelling') and P5/11 ('Mobile multimedia communication systems and networks'), the Concerted Research Action GOA-MEFISTO-666 (Mathematical Engineering for Information and Communication Systems Technology) of the Flemish Government, Research Project FWO nr.G.0196.02 ('Design of efficient communication techniques for wireless time-dispersive multi-user MIMO systems') and was partially sponsored by Alcatel-Bell and Alcatel-MicroElectronics. The scientific responsibility is assumed by its authors.

Bitrate-Maximizing Time-Domain Equalizer Design for DMT-Based Systems

Koen Vanbleu, *Student Member, IEEE*, Geert Ysebaert, *Student Member, IEEE*, Gert Cuypers, *Student Member, IEEE*, Marc Moonen, *Member, IEEE*, and Katleen Van Acker

***Abstract*—A time-domain equalizer (TEQ) is inserted in discrete multitone (DMT) receivers to impose channel shortening. Many algorithms have been developed to initialize this TEQ, but none of them really optimizes the bitrate. We present a truly *bitrate-maximizing* TEQ (BM-TEQ) cost function that is based on an exact formulation of the subchannel signal-to-noise ratio as a function of the TEQ taps. The performance of this BM-TEQ comes close to the performance of the per-tone equalizer.**

***Index Terms*—Asymmetric digital subscriber line (ADSL), discrete multitone (DMT), equalization, time-domain equalizer (TEQ).**

I. Introduction

DISCRETE MULTITONE (DMT) is an all-digital multicarrier modulation scheme adopted for asymmetric digital subscriber line (ADSL) and proposed for very-high-bitrate digital subscriber line (VDSL). The (de)modulation is done with an (inverse) fast Fourier transform ((I)FFT). Before transmission of a DMT symbol, a cyclic prefix of ν samples is added to simplify the equalization. Practical DSL channel impulse responses can be very long. An existing solution to avoid a cyclic prefix with as many samples as the channel impulse response length is to insert a T-tap time-domain equalizer (TEQ) before demodulation that shortens the channel impulse response to $\nu+1$ samples. Many algorithms have been developed to initialize this TEQ, but none of them truly optimizes bitrate.

Minimum mean-square error (MMSE) based methods, such as in [1] and [2], minimize the time-domain error between the TEQ output and a desired output, i.e., the output of a finite-impulse response (FIR) filter of length $\nu+1$, called target-impulse response (TIR), fed with the transmitted time-domain sequence. The TIR is part of the parameter vector. A nontriviality constraint is needed to avoid the trivial all-zero solution. However, minimizing the *time*-domain error energy does not optimize the bitrate, which is based on signal-to-noise ratios (SNRs) in the *frequency* domain.

A computationally efficient generalization of the "maximum shortening-SNR" (MSSNR) method is presented in [3], called "minimum-intersymbol interference (ISI) method". The original MSSNR method is described in [4] and aimed at maximizing the ratio of the energy of the channel-impulse response inside a target window of length $\nu+1$ to the energy outside the target window. None of these methods truly optimizes bitrate.

In [5], the authors attempt to maximize bitrate by maximizing an (approximate) geometric SNR. However, several assumptions render the method suboptimal, e.g., each subchannel SNR takes neither intercarrier interference (ICI) and ISI of the DMT signal nor discrete Fourier transform (DFT) leakage of the external noise into account. Acknowledging this fact, improved subchannel SNR formulations are given in [3], [6], and [7], but there also desired signal, ISI/ICI, and/or DFT leakage are only partially included.

In [8], the authors propose an alternative equalization scheme that maximizes the bitrate per tone, hence the overall bitrate. Equalization is done for each tone separately after the FFT demodulation, hence the term "per-tone equalization" (PTEQ). The PTEQ performs at least as well as, and usually better than, any TEQ-based receiver, while keeping complexity during data transmission at the same level. The drawback of the PTEQ is its memory requirement: N_aT taps (with N_a the number of active tones, e.g., over 200 in downstream ADSL) need to be stored, instead of the T taps in the case of a TEQ.

In this letter, we present a TEQ design criterion that has as its optimal solution the *bitrate-maximizing TEQ* (BM-TEQ) for a given number of taps T. The derivation of the BM-TEQ criterion, which appears to be nonlinear and nonconvex, is given in Section II. The key element in the derivation is the observation that the dependence of the subchannel SNR on the TEQ taps $\mathbf{w}$ is easily accounted for when considering a subchannel SNR formulation at the frequency-domain equalizer (FEQ) *output*. In [3] and [5]–[7], the subchannel SNR is rather considered at the FEQ *input*, i.e., the FFT output, and (larger or smaller) approximations are introduced in the SNR model, as described above. The simulations in Section III show that the BM-TEQ, obtained with either an iterative or recursive nonlinear optimization algorithm, outperforms the above-mentioned TEQs and approaches the performance of the PTEQ with T taps per tone very closely.

Paper approved by N. Al-Dhahir, the Editor for Space–Time, OFDM, and Equalization of the IEEE Communications Society. Manuscript received September 10, 2002; revised February 10, 2003 and October 28, 2003. This work was carried out at the ESAT laboratory of the Katholieke Universiteit Leuven, under the framework of the Belgian State, Prime Minister's Office: Federal Office for Scientific, Technical and Cultural Affairs, Interuniversity Poles of Attraction Programme (2002–2007) IUAP P5/22 and P5/11, under the Concerted Research Action GOA-MEFISTO-666 of the Flemish Government, under Research Project FWO G.0196.02, and was supported in part by Alcatel-Bell. The scientific responsibility is assumed by its authors. This paper was presented in part at the IEEE International Conference on Communications, Anchorage, AK, May 2003.

K. Vanbleu, G. Ysebaert, G. Cuypersis, and M. Moonen are with the Katholieke Universiteit Leuven-ESAT/SCD, B-3001 Leuven-Heverlee, Belgium (e-mail: koen.vanbleu@esat.kuleuven.ac.be; geert.ysebaert@esat.kuleuven.ac.be; gert.cuypers@esat.kuleuven.ac.be; marc.moonen@esat.kuleuven.ac.be).

K. Van Acker is with Research and Innovation, Alcatel Bell, B-2018 Antwerpen, Belgium (e-mail: katleen.van_acker@alcaltel.be).

Digital Object Identifier 10.1109/TCOMM.2004.829564

0090-6778/04$20.00 © 2004 IEEE

II. The BM-TEQ

In the derivation toward a BM-TEQ cost function, we start from the same bitrate expression[1] as in [5]. The total number of bits transmitted in one DMT symbol is given by

$$b_{\mathrm{DMT}} = \sum_{n \in \mathcal{S}_a} \log_2 \left(1 + \frac{\mathrm{SNR}_n}{\Gamma_n}\right) \tag{1}$$

where $\mathcal{S}_a$ is the set of N_a active tones, SNR_n represents the SNR on tone n, and Γ_n is the gap between SNR_n and the SNR required to achieve Shannon capacity. Γ_n is a function of the desired probability of error, coding gain, and system margin. The most advanced coding schemes are able to reduce Γ_n to close to 1 (0 dB). Note that after equalizer design, an integer number of bits is allocated to each tone, incorporating some (possibly iterative) tweaking of the ratios $(\mathrm{SNR}_n/\Gamma_n)$ to optimize the transmit power per tone.

A. An Exact Subchannel SNR Model

When deriving a BM-TEQ design criterion, it is crucial that the dependence of the subchannel SNR_n on the TEQ $\mathbf{w}$ is accurately taken into account. The SNR on tone n can be written formally as

$$\mathrm{SNR}_n = \frac{E_s[n]}{E_e[n]} \tag{2}$$

where $E_s[n]$ is the desired received signal energy on tone n and $E_e[n]$ is the energy in the error signal on tone n, i.e., the received signal less the desired received signal, both on tone n. The signal energy portions $E_s[n]$ and $E_e[n]$ in the subchannel SNR model (2), as it is assumed in [3] and [5]–[7], are determined *at the FFT output*, i.e., the FEQ input. Define the nth FFT output as

$$Y_{k,w}[n] = \mathcal{F}_n \mathbf{Y}_k \mathbf{w} = B_{n,w} X_k[n] + \underbrace{\tilde{I}_{k,w}[n] + \tilde{N}_{k,w}[n]}_{\tilde{E}_{k,w}[n]} \tag{3}$$

where $\mathcal{F}_n$ is the nth row of the $N \times N$ DFT matrix, $\mathbf{w}$ is a $T \times 1$ column vector with the TEQ taps, and $\mathbf{Y}_k$ is a Toeplitz matrix (of size $N \times T$) of received samples[2] $y_k[l]$ (k is the DMT symbol index)

$$\mathbf{Y}_k = \begin{bmatrix} y_k[0] & \cdots & y_k[-T+1] \\ \vdots & \ddots & \vdots \\ y_k[N-1] & \cdots & y_k[N-T] \end{bmatrix}. \tag{4}$$

The matrix-vector product $\mathbf{Y}_k\mathbf{w}$ in (3) calculates the convolution of the kth received DMT symbol and the TEQ; the resulting $N \times 1$ TEQ output vector is fed to the FFT. The nth FFT output $Y_{k,w}[n]$ in (3) is the sum of:

- the desired signal, i.e., a scaled version of the transmitted symbol of interest $X_k[n]$ (tone n, time k, energy $\sigma_X^2[n]$), with complex scalar $B_{n,w}$ (where the subscript w denotes the dependence on the TEQ $\mathbf{w}$);
- plus a noise term $\tilde{E}_{k,w}[n]$ that depends on the TEQ $\mathbf{w}$ and consists of residual ISI/ICI $\tilde{I}_{k,w}[n]$ as well as external noise $\tilde{N}_{k,w}[n]$ (thermal noise, crosstalk, residual echo, narrowband interference, etc.).

Using (3), the signal energies $E_s[n]$ and $E_e[n]$ in the subchannel SNR (2) of [3] and [5]–[7] can be written as

$$\begin{aligned} E_s[n] &= \mathcal{E}\left\{|B_{n,w}X_k[n]|^2\right\} = |B_{n,w}|^2\sigma_X^2[n] \\ E_e[n] &= \mathcal{E}\left\{\left|\tilde{E}_k[n]\right|^2\right\} = \sigma_{\tilde{E},w}^2[n] = \sigma_{\tilde{I},w}^2[n] + \sigma_{\tilde{N},w}^2[n] \end{aligned} \tag{5}$$

where compact notation for variances σ has been introduced. Each of the subchannel SNR models (2) assumed in [3] and [5]–[7] contains a (smaller or larger) *approximation* in one or more of the TEQ-dependent terms in (5), rendering the presented TEQ design not truly bitrate maximizing. The most accurate, approximate SNR models have been introduced in [6] (when combined with [9] to model the ISI/ICI) and [7].[3]

In contrast with [3] and [5]–[7], we prefer to consider the energies $E_s[n]$ and $E_e[n]$ in (2) *at the FEQ output*, as this will provide us with a convenient way of modeling $E_s[n]$ and $E_e[n]$ *without approximation*. This is equally valid, as the FEQs do not alter SNR_n, in the sense that they equally scale both the desired and error signal, hence, both the numerator $E_s[n]$ and denominator $E_e[n]$ in (2). This effectively makes the FEQs showing up in the subchannel SNR model (2). However, as will be shown, the FEQs depend in an elegant way on the TEQ, hence, the FEQs can be written as a function of the TEQ. In the end, we obtain a subchannel SNR model (2) and an optimization criterion (1) that solely depend on the TEQ $\mathbf{w}$.

When designing a linear equalizer such as an FEQ, typically a choice is made between an MMSE and zero-forcing (ZF) equalizer (ZFE). In [11] and [12], it is explained that the traditional *unconstrained MMSE equalizer* is *biased*, hence, it is preferable to turn it into an *unbiased MMSE equalizer*. An unbiased MMSE equalizer gives an unbiased desired signal part at the equalizer output, resulting in minimum probability of error. In general, a ZFE, if existing, is also unbiased, but has a lower SNR because of noise enhancement. In case of a one-tap equalizer, such as the FEQs in a DMT system, there is no noise enhancement, hence, the ZF FEQ and unbiased MMSE FEQ (uMMSE FEQ) are equal[4] ([1, p. 320]), and so will be our FEQ of choice. The FEQ output can be written as

$$D_n \underbrace{\mathcal{F}_n \mathbf{Y}_k \mathbf{w}}_{Y_{k,w}[n]} = \beta_n X_k[n] + \underbrace{I_{k,w}[n] + N_{k,w}[n]}_{E_{k,w}[n]} \tag{6}$$

where D_n is the nth FEQ, $Y_{k,w}[n]$ is the nth FFT output, $\beta_n X_k[n]$ is a scaled version of the transmitted symbol $X_k[n]$, and the error $E_{k,w}[n] = D_n\tilde{E}_{k,w}[n]$ is the sum of residual ISI/ICI $I_{k,w}[n]$ and noise $N_{k,w}[n]$ at the nth FEQ output. The scalar β_n in (6) is 1, i.e., the desired signal component at the FEQ output is unbiased, in the case of uMMSE FEQs D_n

$$D_n = \frac{\sigma_X^2[n]}{\mathcal{E}\left\{X_k^*[n]Y_{k,w}[n]\right\}} = \frac{\sigma_X^2[n]}{\mathcal{E}\left\{X_k^*[n]\mathbf{Y}_{k,sl}[n]\right\}\mathbf{w}}. \tag{7}$$

[1] We do not consider the mathematically much more difficult case of integer bit loading.

[2] It is tacitly assumed that $\mathbf{Y}_k$ depends on the synchronization delay Δ, a design parameter that estimates the channel group delay [2].

[3] Note that an *exact* way of modeling the ISI/ICI term $\bar{I}_{k,w}[n]$ in (3) was first given in [10].

[4] In fact, the ZF FEQ only exists if the channel-impulse response length is not larger than $\nu + 1$, while the uMMSE FEQ always exists.

We included explicitly the dependence of the FEQ D_n on $\mathbf{w}$ in (7) by exploiting the key observation that the nth FFT output can be obtained in two ways

$$Y_{k,w}[n] = \underbrace{\mathcal{F}_n(\mathbf{Y}_k\mathbf{w})}_{[1]} = \underbrace{(\mathcal{F}_n\mathbf{Y}_k)\mathbf{w}}_{[2]} = \mathbf{Y}_{k,sl}[n]\mathbf{w} \quad (8)$$

i.e., [1] as the nth FFT coefficient of the TEQ output $\mathbf{Y}_k\mathbf{w}$ (as explained before), or [2] alternatively, as a linear combination $\mathbf{w}$ of $\mathbf{Y}_{k,sl}[n] = \mathcal{F}_n\mathbf{Y}_k$, a $1\times T$ vector with the outputs on tone n of a sliding DFT of the unequalized signal $y_k[l]$

$$\left(\bar{\mathbf{Y}}_{k,sl}[n]\right)^T = \underbrace{\begin{bmatrix} \boxed{\mathcal{F}_n} & \cdots & 0 \\ \ddots & \ddots & \ddots \\ 0 & \cdots & \boxed{\mathcal{F}_n} \end{bmatrix}}_{\mathbf{F}_n} \begin{bmatrix} y_k[-T+1] \\ \vdots \\ y_k[N-1] \end{bmatrix} \quad (9)$$

where the upper bar reverses the elements of $\mathbf{Y}_{k,sl}[n]$. An efficient, recursive implementation of (9) for all N_a tones requires, per DMT symbol, 1 FFT and $4N_a(T-1)$ real multiplications [8].

With uMMSE FEQs, the desired signal energy $E_s[n]$ becomes independent of TEQ and FEQ, and equals $\sigma_X^2[n]$. The error energy $E_e[n]$ is the mean-square error $\mathcal{E}\{|E_{k,w}[n]|^2\} = \sigma_{E,w}^2[n]$ at the FEQ output, and takes residual ISI/ICI and *all* external noise sources into account. Moreover, (2) is suited for an arbitrary transmit power-allocation scheme. An *exact* subchannel SNR model (2) can thus be written as

$$\mathrm{SNR}_n = \frac{E_s[n]}{E_e[n]} = \frac{\sigma_X^2[n]}{\sigma_{E,w}^2[n]} = \frac{\sigma_X^2[n]}{\mathcal{E}\left\{\left|D_n\mathbf{Y}_{k,sl}[n]\mathbf{w} - X_k[n]\right|^2\right\}}. \quad (10)$$

Introducing compact notation for the $1\times T$ correlation vectors $\Sigma_{X\mathbf{Y}}[n] = \mathcal{E}\{X_k^*[n]\mathbf{Y}_{k,sl}[n]\}$ and $T\times T$ matrices $\Sigma_{\mathbf{Y}}^2[n] = \mathcal{E}\{\mathbf{Y}_{k,sl}^H[n]\mathbf{Y}_{k,sl}[n]\}$, and expanding the denominator of (10) gives

$$\begin{aligned}\sigma_{E,w}^2[n] &= |D_n|^2\mathbf{w}^T\Sigma_{\mathbf{Y}}^2[n]\mathbf{w} - D_n\Sigma_{X\mathbf{Y}}[n]\mathbf{w} \\ &\quad - D_n^*\mathbf{w}^T\Sigma_{X\mathbf{Y}}^H[n] + \sigma_X^2[n] \\ &= \sigma_X^2[n]\left(\frac{\sigma_X^2[n]\left(\mathbf{w}^T\Sigma_{\mathbf{Y}}^2[n]\mathbf{w}\right)}{\left|\Sigma_{X\mathbf{Y}}[n]\mathbf{w}\right|^2} - 1\right) \end{aligned} \quad (11)$$

where the second equation follows from the substitution of the uMMSE FEQs (7). Combining (11) and (10), we obtain a very compact SNR model that only depends on the TEQ $\mathbf{w}$

$$\mathrm{SNR}_n = \frac{\rho_w^2[n]}{1-\rho_w^2[n]} \quad (12)$$

where

$$\rho_w^2[n] = \frac{\left|\Sigma_{X\mathbf{Y}}[n]\mathbf{w}\right|^2}{\sigma_X^2[n]\left(\mathbf{w}^T\Sigma_{\mathbf{Y}}^2[n]\mathbf{w}\right)} \quad (13)$$

$$= \frac{\left|\mathcal{E}\left\{X_k^*[n]Y_{k,w}[n]\right\}\right|^2}{\sigma_X^2[n]\mathcal{E}\left\{\left|Y_{k,w}[n]\right|^2\right\}} \quad (14)$$

$$= \frac{\left|\sigma_{XY,w}[n]\right|^2}{\sigma_X^2[n]\sigma_{Y,w}^2[n]} \quad (15)$$

is a squared normalized correlation function of FFT output $Y_{k,w}[n]$ and symbol $X_k[n]$. The first line (13) and second line (14) are related by the key observation in (8). Compact notation for (co)variances $\sigma_{XY,w}[n]$ and $\sigma_{Y,w}^2[n]$ has been introduced in (15).

B. The BM-TEQ Cost Function

Using (1), (12), and (13), the BM-TEQ is then the solution of

$$\begin{aligned}&\arg\max_{\mathbf{w}} b_{\mathrm{DMT}} \\ &\quad = \arg\max_{\mathbf{w}} \sum_{n\in\mathcal{S}_a} \log\left(1 + \frac{\rho_w^2[n]}{\Gamma_n\left(1-\rho_w^2[n]\right)}\right) \\ &\quad = \arg\min_{\mathbf{w}} \sum_{n\in\mathcal{S}_a} \log\left(\frac{\Gamma_n\left(1-\rho_w^2[n]\right)}{\Gamma_n + (1-\Gamma_n)\rho_w^2[n]}\right) \end{aligned} \quad (16)$$

$$\boxed{\arg\max_{\mathbf{w}} b_{\mathrm{DMT}} = \arg\min_{\mathbf{w}} \sum_{n\in\mathcal{S}_a} \log\left(\frac{\mathbf{w}^T\mathbf{B}_n\mathbf{w}}{\mathbf{w}^T\mathbf{A}_n\mathbf{w}}\right).} \quad (17)$$

$\mathbf{A}_n$ and $\mathbf{B}_n$ are independent of $\mathbf{w}$ and depend on the second-order signal statistics $\sigma_X^2[n]$, $\Sigma_{\mathbf{Y}}^2[n]$ and $\Sigma_{X\mathbf{Y}}[n]$

$$\mathbf{A}_n = \Gamma_n\sigma_X^2[n]\Sigma_{\mathbf{Y}}^2[n] + (1-\Gamma_n)\Sigma_{X\mathbf{Y}}^H[n]\Sigma_{X\mathbf{Y}}[n] \quad (18)$$

$$\mathbf{B}_n = \Gamma_n\left(\sigma_X^2[n]\Sigma_{\mathbf{Y}}^2[n] - \Sigma_{X\mathbf{Y}}^H[n]\Sigma_{X\mathbf{Y}}[n]\right) \quad (19)$$

The choice above to derive the BM-TEQ cost function (17) using uMMSE FEQs (7) provides a convenient way of modeling the numerator $E_s[n]$ and denominator $E_e[n]$ of SNR_n in (2) without approximation. However, as the FEQs equally scale both $E_s[n]$ and $E_e[n]$, and hence do not alter SNR_n, the BM-TEQ cost function (17) remains valid, if the actual FEQs are the unconstrained/biased MMSE FEQs.

Some further remarks:

- As the BM-TEQ criterion (17) does not explicitly impose channel shortening any more, and as at most $N/2+1$ of the N DFT frequency bins are demodulated, one could also use a complex-valued TEQ, giving up the conjugate symmetry at the FFT output. The extra degrees of freedom (the imaginary part of the T taps) result in a slightly better performance than a real-valued TEQ, at the cost of extra computational complexity (e.g., a more complex FFT).
- The solution of the BM-TEQ cost function (17) has a scalar ambiguity. For a solution $\mathbf{w}$, $\gamma\mathbf{w}$ (with γ a scalar) is also a solution, as the FEQ compensates for the scaling by γ. In contrast to MMSE-based TEQ design, imposing a constraint on $\mathbf{w}$, e.g., $\|\mathbf{w}\| = 1$, does not influence the optimum bitrate, as the bitrate b_{DMT} in (17) is independent of the scalar γ.
- The BM-TEQ design is easily combined with a bandwidth-optimization scheme, as presented in [13], that could further improve performance.

C. Solving the BM-TEQ Cost Function

Minimizing (17) is a nonlinear, nonconvex optimization problem. An iterative (batch) as well as a recursive initialization algorithm are proposed below. The nonconvexity makes that both algorithms only assure convergence to a local optimum [14].

Nonlinear *batch-optimization methods* such as advanced, *iterative* (quasi-)Newton and simplex algorithms are implemented in the MATLAB optimization toolbox. Estimates of the crosscorrelation matrices $\Sigma^2_{\mathbf{Y}}[n]$ and vectors $\Sigma_{X\mathbf{Y}}[n]$ for all tones in $\mathcal{S}_a$ can be obtained accurately with the DMT data model of [8], based on an estimate of channel-impulse response and noise statistics, given as

$$\begin{aligned}\begin{bmatrix} y_k[-T+1] \\ \vdots \\ y_k[N-1] \end{bmatrix} &= \underbrace{\left[\begin{array}{c|ccc|c} \mathbf{O}_{(1)} & \bar{\mathbf{h}} & 0 & \cdots & \\ & & \ddots & \ddots & \mathbf{O}_{(2)} \\ & 0 & \cdots & \bar{\mathbf{h}} & \end{array}\right] \cdot (\mathbf{I}_3 \otimes \mathbf{P}) \cdot (\mathbf{I}_3 \otimes \mathcal{F}^H)}_{\mathbf{H}} \\ &\quad \times \underbrace{\begin{bmatrix} X_{k-1} \\ X_k \\ X_{k+1} \end{bmatrix}}_{\mathbf{X}} + \underbrace{\begin{bmatrix} n_k[-T+1] \\ \vdots \\ n_k[N-1] \end{bmatrix}}_{\mathbf{n}} \\ &= \underbrace{\mathbf{H}_{N+n} X_k[n]}_{\text{desired}} + \underbrace{\tilde{\mathbf{H}}\tilde{\mathbf{X}}}_{\text{ISI/ICI}} + \underbrace{\mathbf{n}}_{\text{noise}}. \end{aligned} \tag{20}$$

In (20), $\bar{\mathbf{h}}$ denotes the length-N channel-impulse response with coefficients in reverse order; $\mathbf{O}_{(1)}$ and $\mathbf{O}_{(2)}$ are zero matrices of size $(N+T-1)\times(2\nu+\Delta-T+1)$ and $(N+T-1)\times(N+\nu-\Delta)$, respectively, as part of a $(N+T-1)\times(3(N+\nu))$ Toeplitz channel convolution matrix; ν is the cyclic-prefix length; Δ is the synchronization delay; $\mathbf{I}_n$ is an $n\times n$ identity matrix; $\otimes$ denotes the Kronecker product, and $\mathbf{P}$ is a $(N+\nu)\times N$ matrix that adds the cyclic prefix; and $\mathcal{F}^H$ is the $N\times N$ IDFT matrix. The equivalent channel matrix $\mathbf{H}$ has size $(N+T-1)\times(3N)$; the $3N\times 1$ vector $\mathbf{X}$ contains the transmitted symbols at time $k-1$, k, and $k+1$. $\mathbf{H}_{N+n}$ is the $(N+n)$th column of $\mathbf{H}$ that corresponds to the symbol of interest $X_k[n]$; $\tilde{\mathbf{H}}$ is obtained from $\mathbf{H}$ by omitting the $(N+n)$th column; and $\tilde{\mathbf{X}}$ is obtained from $\mathbf{X}$ by omitting $X_k[n]$. The $(N+T-1)\times(N+T-1)$ (time-domain) noise covariance matrix is given by $\mathcal{E}\{\mathbf{n}\mathbf{n}^T\}$. Then, it follows from (20) and (9) that the required second-order statistics are given by

$$\Sigma^2_{\mathbf{Y}}[n] = \bar{\mathbf{F}}^*_n \left(\mathbf{H}^*\mathbf{S}\mathbf{H}^T + \mathcal{E}\{\mathbf{n}\mathbf{n}^T\}\right)\bar{\mathbf{F}}^T_n \tag{21}$$

$$\Sigma_{X\mathbf{Y}}[n] = \sigma^2_X[n]\mathbf{H}^T_{N+n}\bar{\mathbf{F}}^T_n \tag{22}$$

where $\bar{\mathbf{F}}_n$ is the Toeplitz sliding DFT matrix $\mathbf{F}_n$, defined in (9), with the rows in reverse order, and $\mathbf{S}$ is a diagonal matrix with diagonal elements $\sigma^2_X[n]$ for the active tones and 0 for nonactive tones. Alternatively, one can estimate these statistics (21) and (22) using the training sequence (with cyclic prefix) that is transmitted during the connection setup.

In the simulations of Section III, we use a *recursive initialization* algorithm based on a stochastic Newton algorithm with Gauss–Newton-like search direction [14]. The algorithm uses recursive estimates of all matrices $\Sigma^2_{\mathbf{Y}}[n]$ and vectors $\Sigma_{X\mathbf{Y}}[n]$ in the gradient, and the positive-semidefinite Hessian approximation to update $\mathbf{w}$ for each new DMT symbol. This recursive algorithm also allows for further adaptation and tracking during data transmission. An efficiently implemented update requires one FFT and on the order of $O(N_aT^2)+O(T^3)$ multiplications per DMT symbol (T is the number of TEQ taps, N_a is the number of active tones). An algorithm description and detailed complexity analysis is beyond the scope of this letter.

III. Simulations

Although the BM-TEQ cost function (17) is nonlinear and nonconvex, simulations with both the iterative and recursive algorithm with random initialization converge to locally optimal TEQs with a corresponding bitrate that differs by less than 6 kb/s. The recursive algorithm converges very quickly (a good estimate for $\mathbf{w}$ is obtained after less than 100 updates). We compare the BM-TEQ (with recursive initialization) with the PTEQ [8] and with other TEQ designs, such as the MMSE-based design with unit norm and unit tap constraint on the TIR $\mathbf{b}$ [1], [2], the maximum bitrate (MBR) and minimum-ISI approach [3], the approximate geometric SNR (AGSNR) design (with suboptimal SNR_n) in [5], and the TEQ design by Henkel *et al.* (referred to below with "HBM-TEQ design") [6], [9]. The MBR-TEQ optimization is implemented as in the MATLAB DMT-TEQ Design Toolbox [15] and initialized with the minimum-ISI TEQ for each Δ, as suggested in [3]. The AGSNR design starts from a target impulse response $[1\ 1\ldots 1]$, as suggested in [5]. The parameter $\mathrm{MSE}_{\max}$ in the AGSNR TEQ design is optimized over the range between its lower and upper bound, derived in [5] and [13]. The HBM-TEQ optimization is initialized with an MMSE-based TEQ, as is suggested in [6].

The bitrate calculation requires an estimate of SNR_n per tone n. The noise energy $\sigma^2_{E,w}[n]$ in (10) is estimated, after the equalizer design, as a 1024-point average of the square of the residual noise $E_{k,w}[n]$ at the uMMSE FEQ output (6). The bitrates depicted below are based on constellations with an integer number of bits.

Three ADSL scenarios are presented: an upstream and two downstream simulations, all with the carrier-serving area (CSA) loop 4. They are representative of simulations with other CSA loops. The CSA4 loop is a 7600-ft, 26-gauge loop with two 26-gauge bridged taps, one of length 400 ft at 550 ft and one of length 800 ft at 6800 ft [3], [5]. The DMT transmit power on the active tones is -40 dBm/Hz. The noise includes additive white Gaussian background noise (-140 dBm/Hz), residual echo, and near-end and far-end crosstalk (NEXT and FEXT) coming from 24 ADSL disturbers, as described in [16].

Fig. 1 shows the bitrate as a function of the number of TEQ taps for a downstream CSA4 loop, with no other front-end filter (analog or digital) than the plain old telephone service (POTS) splitter. The active tones are tones 7–256; it is assumed that echo from upstream signaling is perfectly cancelled. The synchronization delay Δ has been optimized over the values 2, 6, ..., 58. The maximum energy window[5] starts at sample 28. There is

[5]This window contains the $\nu+1$ consecutive channel impulse response samples with maximum energy.

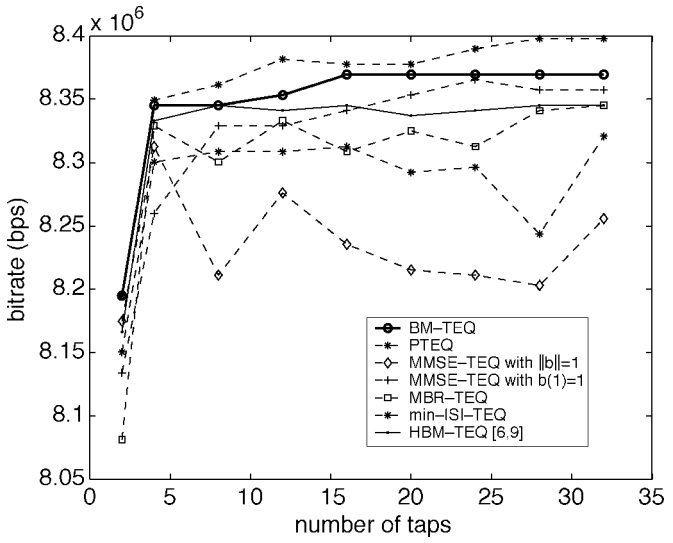

Fig. 1. Bitrate as a function of the number of TEQ taps for the *downstream* CSA4 loop *without* analog and digital front-end filters (except POTS splitter). The synchronization delay Δ has been optimized over the values 2, 6, . . ., 58.

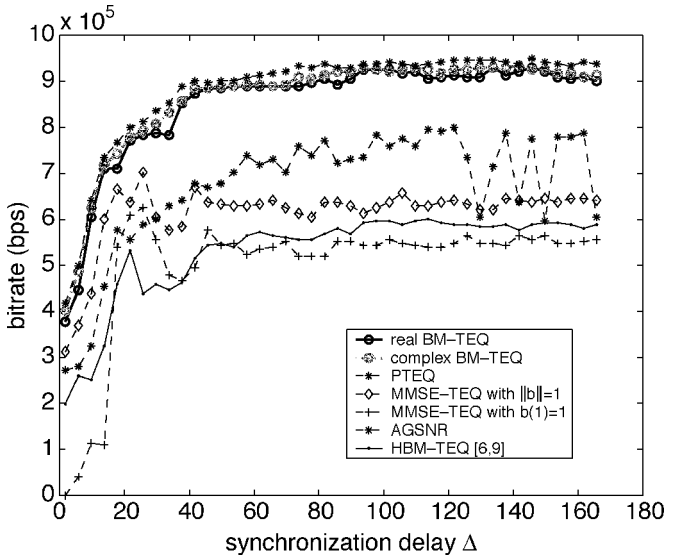

Fig. 2. Bitrate as a function of synchronization delay Δ for the *upstream* CSA4 loop *with* analog and digital front-end filters. Number of taps $T = 44$.

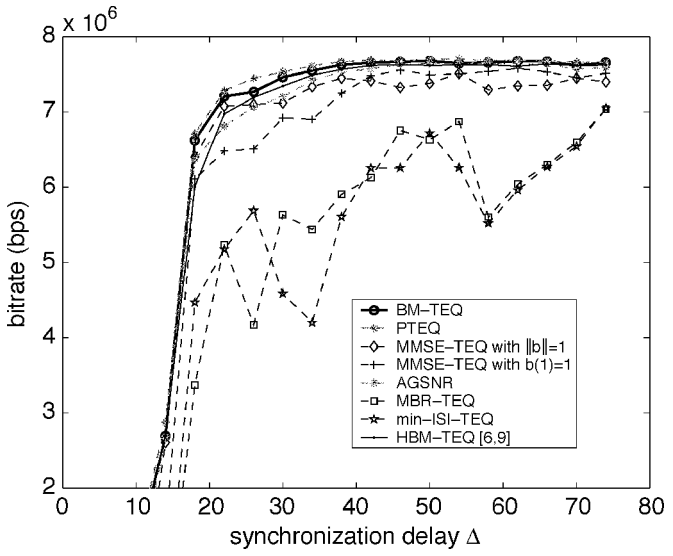

Fig. 3. Bitrate as a function of synchronization delay Δ for the *downstream* CSA4 loop *with* analog and digital front-end filters. Number of taps $T = 32$.

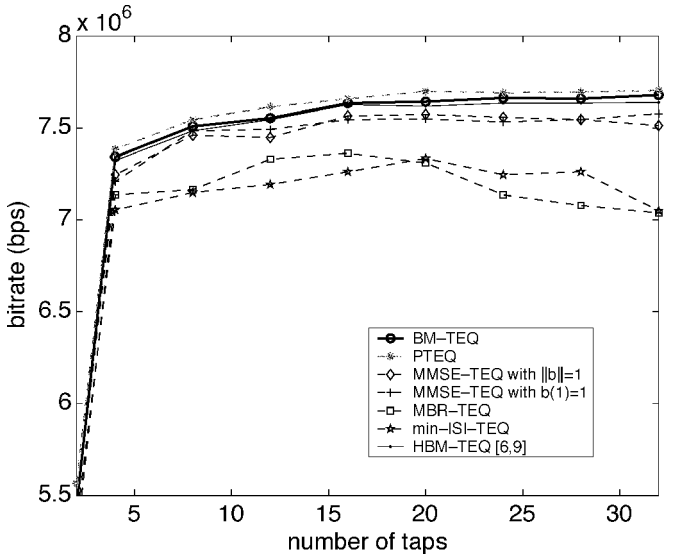

Fig. 4. Bitrate as a function of the number of TEQ taps for the *downstream* CSA4 loop *with* analog and digital front-end filters. The synchronization delay Δ has been optimized over the delay values 6, 10, . . ., 74.

only a 4% difference in bitrate between a "poorly" performing TEQ with two taps and a PTEQ with 32 taps. The reason for this small difference between the studied TEQ designs is the absence of most of the front-end filters. These filters are needed in a frequency-division duplexing (FDD) setup to separate upstream and downstream. The filters introduce a considerable amount of ISI/ICI near the band edges [10]. Hence, a larger number of taps is needed and the performance difference between the equalizer designs becomes clearer.

Fig. 2 shows the bitrate as a function of synchronization delay Δ for a TEQ of 44 taps in the *upstream* CSA4 simulation. Now, analog and digital FDD front-end filters have been included. Tones 8–32 carry information. The transmit IFFT size is 512 and the receiver FFT size is 128. The maximum energy window starts at sample 38. The real and complex BM-TEQs outperform all other TEQ algorithms.[6] Its bitrate is smooth as a function of Δ and approaches the PTEQ performance. The AGSNR approach outperforms the MMSE-based TEQ designs for most delays but, due to its suboptimal subchannel SNR, it stays away from the BM-TEQ.

Fig. 3 shows the bitrate as a function of synchronization delay for a TEQ of 32 taps in the *downstream* CSA4 simulation with front-end filters. The tones 38–256 are used. Both IFFT and FFT have size 512. The maximum energy window starts at sample 46. Again, the BM-TEQ outperforms the other TEQs and has almost the same performance as the PTEQ. Among the other TEQ designs, the MMSE-based TEQ and AGSNR designs per-

[6]The minimum-ISI TEQ method is not directly applicable, as the number of taps $(T = 44)$, which is larger than the number of upstream tones $(N_u = 25)$ and the cyclic-prefix length $(\nu = 8)$, renders matrices in the cost function rank deficient.

form well, and the HBM-TEQ design approaches very closely the BM-TEQ performance.

Fig. 4 shows the bitrate as a function of the number of taps for the same downstream scenario. The synchronization delay Δ has been optimized over the delay values 6, 10, ..., 74. Only the BM-TEQ and PTEQ perform consistently better for an increasing number of taps; the HBM-TEQ design almost does. The other designs do not, because they do not optimize the true bitrate.

IV. Conclusions

We have presented a new nonlinear cost function for TEQ design that maximizes the bitrate (BM-TEQ). The derivation of the BM-TEQ cost function is based on a subchannel SNR model at the FEQ output, as this helps to take the dependence of the SNR on the TEQ into account without any approximation. A recursive stochastic Newton algorithm is suggested to initialize the TEQ, as this typically results in fast convergence. Simulations confirm the superior performance of the BM-TEQ, compared with other TEQs. Its performance comes close to the PTEQ performance while strongly reducing memory requirements.

Acknowledgment

We would like to thank the anonymous reviewers for their thorough reading and valuable comments.

References

[1] T. Starr, J. Cioffi, and P. Silvermann, *Understanding Digital Subscriber Line Technology*. Englewood Cliffs, NJ: Prentice-Hall, 1999.

[2] N. Al-Dhahir and J. Cioffi, "Efficiently computed reduced-parameter input-aided MMSE equalizers for ML detection: A unified approach," *IEEE Trans. Inform. Theory*, vol. 42, pp. 903–915, May 1996.

[3] G. Arslan, B. Evans, and S. Kiaei, "Equalization for discrete multitone transceivers to maximize bit rate," *IEEE Trans. Signal Processing*, vol. 49, pp. 3123–3135, Dec. 2001.

[4] P. Melsa, R. Younce, and C. Rohrs, "Impulse response shortening for discrete multitone transceivers," *IEEE Trans. Commun.*, vol. 44, pp. 1662–1672, Dec. 1996.

[5] N. Al-Dhahir and J. Cioffi, "Optimum finite-length equalization for multicarrier transceivers," *IEEE Trans. Commun.*, vol. 44, pp. 56–64, Jan. 1996.

[6] W. Henkel and T. Kessler, "Maximizing the channel capacity of multicarrier transmission by suitable adaptation of the time-domain equalizer," *IEEE Trans. Commun.*, vol. 48, pp. 2000–2004, Dec. 2000.

[7] M. Milosevic, L. F. C. Pessoa, B. L. Evans, and R. Baldick, "Optimal time-domain equalization design for maximizing data rate of discrete multitone systems," *IEEE Trans. Signal Processing*, to be published.

[8] K. Van Acker, G. Leus, M. Moonen, O. van de Wiel, and T. Pollet, "Per-tone equalization for DMT-based systems," *IEEE Trans. Commun.*, vol. 49, pp. 109–119, Jan. 2001.

[9] W. Henkel, G. Tauböck, P. Ödling, P. Börjesson, and N. Petersson, "The cyclic prefix of OFDM/DMT—An analysis," in *Proc. Int. Zurich Seminar Broadband Communications*, Feb. 2002, pp. 22-1–22-3.

[10] T. Pollet, H. Steendam, and M. Moeneclaey, "Performance degradation of multicarrier systems caused by an insufficient guard-interval duration," in *Proc. Int. Workshop Copper Wire Access Systems "Bridging the Last Copper Drop"*, Budapest, Hungary, Oct. 1997, pp. 265–270.

[11] J. Cioffi, G. Dudevoir, M. Eyuboglu, and G. Forney, Jr., "MMSE decision-feedback equalizers and coding—Part I: Equalization results," *IEEE Trans. Commun.*, vol. 43, pp. 2582–2594, Oct. 1995.

[12] E. de Carvalho and D. Slock, "Burst mode equalization: Optimal approach and suboptimal continuous-processing approximation," *Signal Processing*, vol. 80, pp. 1999–2015, Oct. 2000.

[13] N. Al-Dhahir and J. Cioffi, "A bandwidth-optimized reduced-complexity equalized multicarrier transceiver," *IEEE Trans. Commun.*, vol. 45, pp. 948–956, Aug. 1997.

[14] L. Ljung and T. Söderström, *Theory and Practice of Recursive Identification*. Cambridge, MA: MIT Press, 1983.

[15] Embedded Signal Processing Lab., Univ. Texas at Austin. TEQ Design Toolbox. [Online]. Available: http://www.ece.utexas.edu/~bevans/projects/adsl/dmtteq/dmtteq.html

[16] "ITU Recommendation G.996.1. Test Procedures for Digital Subscriber Line (DSL) Transceivers," Int. Telecommun. Union, Geneva, Switzerland, Feb. 2001.